Applied Catalysis B: Environmental 168-169 (2015) 98–104

Contents lists available at ScienceDirect

Applied Catalysis B: Environmental

journal homepage: www.elsevier.com/locate/apcatb

One silver(I)/tetraphosphine coordination polymer showing good catalytic performance in the photodegradation of nitroaromatics in aqueous solution

Xin-Yi Wu [a], Hai-Xiao Qi [a], Jin-Jiao Ning [a], Jian-Feng Wang [a], Zhi-Gang Ren [a,*], Jian-Ping Lang [a,b,*]

[a] College of Chemistry, Chemical Engineering and Materials Science, Soochow University, Suzhou 215123, People's Republic of China
[b] State Key Laboratory of Organometallic Chemistry, Shanghai Institute of Organic Chemistry, Chinese Academy of Sciences, Shanghai 200032, People's Republic of China

ARTICLE INFO

Article history:
Received 8 August 2014
Received in revised form
13 December 2014
Accepted 16 December 2014
Available online 18 December 2014

Keywords:
Silver(I)
Coordination polymer
Catalyst
Photodegradation
Nitroaromatics

ABSTRACT

Reaction of $AgNO_3$ with one tetraphosphine ligand, 1,4-*N*,*N*,*N*′,*N*′-tetra(diphenylphosphanylmethyl) benzene diamine (dpppda), gave rise to a Ag(I)/tetraphosphine coordination polymer $[Ag_4(NO_3)_4(dpppda)]_n$ (**1**). Compound **1** has a one-dimensional (1D) chain structure in which the chair-like $[Ag_4(NO_3)_4]$ cores are linked by the dpppda ligands using a Z-shaped μ-η^2:η^2 side-by-side mode. Compound **1** exhibited good catalytic activity towards the photodegradation of nitrobenzene (NB), paranitrophenol (PNP) and 2,4-dinitrophenol (2,4-DNP) in aqueous solution under UV light irradiation. The kinetics and the mechanism of such catalytic photodegradation reactions were also investigated. The present work provided some new insight into the design and preparation of new coordination polymers as catalyst for high-performance photodegradation of toxic and persistent organic species existed in industrial wastewaters.

1. Introduction

In the past decades, industrial wastewaters have become one of the most serious problems related to our human environment [1]. Among them, nitroaromatics such as nitrobenzene (NB) and nitrophenol (NP) are commonly encountered, and toxic and persistent. Even at low concentrations, NB or NP may pose a high risk to the environment and human health [2–6]. General methods for treating the industrial wastewaters include ozonation, adsorption and biodegradation, which are not environmentally friendly and relatively expensive due to the fact that these methods require further treatments and may lead to the secondary pollution [7–10]. Catalytic photodegradation is a promising technique for the treatment and purification of such wastewaters as it could completely mineralize organic pollutants into harmless inorganic compounds [11–17]. Currently, semiconductor compounds such as metal oxides (e.g. TiO_2, ZnO, WO_3, SnO_2, ZrO_2), metal sulfides (e.g. CdS and ZnS) and metal or non-metal-doped composites are frequently employed as catalysts for the photodegradation reactions [18–30]. For example, Priya et al. reported that a series of nitrobenzenes could be photodegraded to less than 10% of their original concentrations within 2–3 h by using nano TiO_2 as a catalyst [18].

Apart from those semiconductors, in recent years, some metal coordination compounds such as $\{[Cu^{II}(SalImCy)](Cu^{I}I)_2 \cdot DMF\}_n$ (SalImCy = *N*,*N*′-bis-[(imidazol-4-yl)methylene]cyclohexane-1,2-diamine) [31], $[Mn_2(pytpy)_{4/3}(pbcppy)_2]$ (pytpy = 4′-(4-pyridyl)-4,2′:6′,4″-terpyridine; pbcppy = 4-phenyl-2,6-bis(4-carboxyphenyl)pyridine) [32], $[Cu(dmbimdz)]_n$ (dmbimdz = 5,6-dimethyl benzimidazolate) [33] and $[Ni(pytpy)_2Mo_4O_{13}]_n$ [34] have also been reported to be active in catalyzing the photodegradation of organic dyes [31–45]. For the silver-containing compounds, there have been mainly nanoparticles, simple salts and composite materials that are used as catalysts for the photodegradation reactions [46–51]. Only a very few Ag(I) coordination compounds have been utilized as catalysts for decomposing organic dyes like methylene blue (MB) [37,41,51]. This is because Ag(I) coordination compounds are usually sensitive to light and water. For instance, Wałęsa-Chorab reported that a dinuclear helical Ag(I) complex could catalyze the photodegradation of MB with up to 90% efficiency [51]. However its practicability was limited due to its long

* Corresponding authors at: College of Chemistry, Chemical Engineering and Materials Science, Soochow University, Suzhou, 215123, People's Republic of China. Tel.: +86 512 65882865; fax: +86 512 65880328.
E-mail address: jplang@suda.edu.cn (J.-P. Lang).

http://dx.doi.org/10.1016/j.apcatb.2014.12.024
0926-3373/

photoreaction time (9 h) and non-recyclability. To our knowledge, no metal coordination compounds have been employed as catalysts for the photodecomposition of nitroaromatics so far.

We have been interested in the construction of coordination polymers derived from metal ions and bridging N- or P- donor ligands [52–58]. Some of them could efficiently catalyzing the photodegradation of organic dyes [43,44]. These preliminary results activated us to attempt these coordination compounds to catalytically photodecompose nitroaromatics such as NB and NP in aqueous solutions. The Ag(I) complexes of polyphosphine ligands attracted our attention because the rich coordination sites of these ligands could greatly stabilize the Ag(I) ions by forming insoluble and less light - and water- sensitive coordination polymers [52–55]. Thus a tetraphosphine ligand, 1,4-*N*,*N*,*N*′,*N*′-tetra(diphenylphosphanylmethyl) benzene diamine (dpppda) [59], was selected to react with $AgNO_3$ to produce a 1D coordination polymer $[Ag_4(NO_3)_4(dpppda)]_n$ (**1**). Complex **1** was revealed to exhibit good catalytic activity towards the photodegradation of three different nitoaromatics including nitrobenzene (NB), paranitrophenol (PNP) and 2,4-dinitrophenol (2,4-DNP) in aqueous solution. This catalyst could be recycled for at least five times to maintain its high catalytic efficiency. In addition, the mechanism for the catalytic photodegradation of these nitroaromatics was also studied. Described below are the preparation, characterization and catalytic photodegradation performance of **1**.

2. Experimental

2.1. General procedures

The ligand dpppda was prepared according to literature method [59]. All organic solvents were pre-dried over activated molecular sieves and refluxed over the appropriate drying agents under argon. Other chemicals were obtained from commercial sources and used as received. Elemental analyses for C, H and N were performed on a Carlo-Erba CHNO-S microanalyzer. The IR spectrum was recorded on a Varian 1000 FT-IR spectrometer as KBr disks (4000–400 cm^{-1}). The ^1H and $^{31}P\{^1H\}$ NMR spectra were recorded at ambient temperature on a Varian UNITY plus-400 spectrometer. Chemical shifts were referenced to the solvent signal in DMSO-d_6 (^1H). The UV–vis absorption spectra of NB, PNP and 2,4-DNP aqueous solutions were measured on a Varian Cary-50 UV–vis spectrophotometer. The solid-state optical diffuse-reflection spectra were measured on a Shimadzu UV-3150 spectrometer at room temperature in the range of 200–800 nm.

2.2. Synthesis of $[Ag_4(NO_3)_4(dpppda)]_n$ (*1*)

To a solution of $AgNO_3$ (7 mg, 0.04 mmol) in MeCN (5 mL) was added a solution of dpppda (9 mg, 0.01 mmol) in MeCN (5 mL). The resulting mixture was stirred for 30 min and filtered. Diethyl ether (40 mL) was layered onto the filtrate at ambient temperature for 2 days to form yellow crystals of **1**, which were collected by filtration, washed with Et_2O and dried in vacuo. Yield: 11 mg (68% based on dpppda). Anal. Calcd for $C_{58}H_{52}Ag_4N_6O_{12}P_4$: C, 44.05; H, 3.29; N, 5.32%. Found: C, 44.29; H, 3.33; N, 5.26%. IR (KBr disk): 3094 (w), 2359 (m), 2341 (m), 1615 (w), 1514 (s), 1474 (m), 1455 (m), 1434 (s), 1384 (m), 1296 (s), 1212 (w), 1136 (s), 1099 (m), 996 (m), 868 (m), 798 (s), 743 (m), 692(s) cm^{-1}. ^1H NMR (400 MHz, DMSO-d_6, ppm): 7.70–7.40 (m, 40H, -PPh_2), 6.85 (s, 4H,-Ph- in dpppda), 4.37 (s, 8H, -CH_2- in dpppda). ^{31}P NMR (161.9 MHz, DMSO-d_6, ppm): 23.413 (s, 1P, -PPh_2).

2.3. Single-crystal X-ray structure determination

One single crystal of **1** suitable for X-ray analysis was obtained directly from the above preparation. All measurements were made on a Rigaku Mercury CCD X-ray diffractometer by using graphite monochromated Mo *Kα* (λ = 0.71073 Å) radiation. The single crystal was mounted at the top of a glass fiber with grease in a stream of gaseous nitrogen at 223 K. The program CrystalClear (Rigaku and MSC, ver 1.3, 2001) was used for the refinement of cell parameters and the reduction of collected data, while absorption corrections (multi-scan) were applied. The reflection data were also corrected for Lorentz and polarization effects. The crystal structure of **1** was solved by direct methods and refined on F^2 by full-matrix least-squares techniques with SHELXTL-97 program [60,61]. All non-hydrogen atoms were refined anisotropically, while all H atoms were placed in geometrically idealized positions. The crystal data for **1** was summarized as follows: $C_{29}H_{25}O_6N_3Ag_2P_2$, $M_r = 789.20$, $0.32 \times 0.12 \times 0.08$ mm, triclinic, space group $P\bar{1}$, $a = 10.649(2)$ Å, $b = 12.367(3)$ Å, $c = 12.424(3)$ Å, $\alpha = 95.00(3)^\circ$, $\beta = 98.78(3)^\circ$, $\gamma = 107.19(3)^\circ$, $V = 1529.7(5)$ Å^3, $Z = 2$, $D_c = 1.714$ g·cm^{-3}, $F(000) = 784$ and $\mu = 1.431$ mm^{-1}, 6844 reflections collected, 6844 unique ($R_{int} = 0.0942$). $R_1 = 0.0940$, $wR_2 = 0.2952$ and $S = 1.012$.

2.4. Evaluation of the photocatalytic activity

The catalytic photodegradation was carried out in aqueous solution containing the photocatalyst **1** and nitroaromatics (NB, PNP or 2,4-DNP). The solutions of NB, PNP and 2,4-DNP were prepared by stirring the mixture containing each compound and water for 2 h. The water phases were separated and diluted to 5×10^{-4} M for each nitroaromatic (measured by UV spectrophotometer). 20 mg (0.013 mmol) of **1** was carefully grinded and added into 30 mL (0.015 mmol) of each of the above solutions in a 50 mL quartz tube. A BET measurement showed the catalyst **1** used as a powder in the degradation has the BET surface area of 0.57 m^2/g, suggesting that its pore volume **1** is small. Each nitroaromatic could easily achieve the sorption/desorption equilibrium by stirring the above mixture in the dark after 0.5 h (Fig. S1). The resulting suspension was then irradiated by a high pressure Hg lamp (400 W, 365 nm) with no light filter. The lamp and each sample were put in a water bath while the temperature was kept at lower than 35 °C to avoid any temperature effect. The distance between them was adjusted to maintain the light-power density being 30 mW/cm^2. At regular time intervals, 1 mL solution was aspirated, filtered and then diluted to 10 mL by water to measure the residual concentration of the sample by UV spectrophotometer.

2.5. Collection of CO_2 evolved from the photodegradation reaction

As shown in Fig. S2, a 2 mL sample cup containing saturated $Ba(OH)_2$ solution was hung in the reaction tube over the solution containing **1** and NB (30 mL, 5×10^{-4} M). The reaction tube was then filled with pure O_2 and stuffed up by a rubber stopper with an iron wire (Φ 0.5 mm). Upon UV light irradiation, the clear $Ba(OH)_2$ solution gradually became muddy and formed white $BaCO_3$ precipitate at the surface, which was stirred by the iron wire every 15 min to facilitate the reaction between CO_2 and $Ba(OH)_2$. After the irradiation, acetic acid was injected into the reaction solution to convert any CO_3^{2-} into CO_2. The $BaCO_3$ precipitates were finally filtered, washed by water, dried in vacuum at 45 °C and weighed to calculate the yield of CO_2.

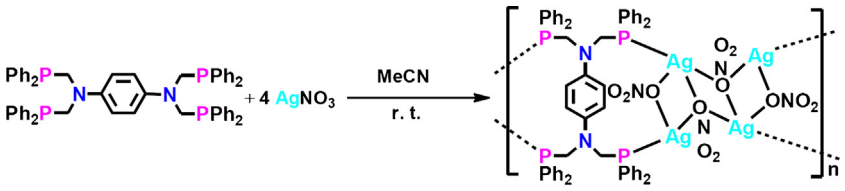

(1)

Scheme 1. Synthesis of **1**.

3. Results and discussion

3.1. Synthesis and structural characterization of *1*

Compound **1** was produced directly from the reaction of dpppda and $AgNO_3$ (molar ratio = 1:4) in MeCN at ambient temperature with 68% yield (Scheme 1). It is stable toward air, moisture and light and soluble in common solvents such as DMSO, DMF and MeCN, but insoluble in water. The elemental analysis of **1** was consistent with its formula. The PXRD patterns of **1** correlated well with the simulated ones generated from the single-crystal X-ray diffraction data (Fig. S3). In the IR spectrum of **1**, the stretching vibrations at 1615/1510 and 1384/868 cm^{-1} were assignable to the phenyl groups and the NO_3^- anions. The ^1H NMR spectrum of **1** in DMSO-d_6 at room temperature showed the signals of dpppda including a multiplet at 7.80–7.43 ppm for the phenyl groups, a singlet at 6.75 ppm for -Ph- group, and a singlet at 4.37 ppm for methylene groups. In the $^{31}P\{^1H\}$NMR of **1**, only one peak (23.413 ppm) was found. The identity of **1** was further confirmed by single-crystal X-ray diffraction analysis. (Scheme 1)

Compound **1** crystallizes in the triclinic space group $P\bar{1}$, and its asymmetric unit contains half of one $[Ag_4(NO_3)_4(dpppda)]$ molecule. There is a crystallographic center of symmetry that lies at the midpoint of Ag1 and Ag1A contact (Fig. 1). Two NO_3^- anions take doubly-bridging and triply-bridging coordination modes, respectively. Ag1 (or Ag1A) is trigonally coordinated by P1 (or P1B), μ-O4 (or O4A) and μ_3-O1 (or O1A) while Ag2 (or Ag2A) is tetrahedrally coordinated by P2B (or P2), μ-O4 (O4A), μ_3-O1 (O1A) and μ_3-O1A (O1). Four Ag(I) centers are joined by four NO_3^- anions to form a chair-like $[Ag_4(NO_3)_4]$ fragment. The Ag1···Ag2 and the Ag1···Ag2A separations are 3.828(2) Å and 3.656(1) Å, which excludes any metal-metal interactions. Each $[Ag_4(NO_3)_4]$ fragment in **1** connects its two equivalent ones via dpppda to form a 1D chain extending along the *a* axis. Each dpppda adopts a Z-shaped μ-η^2:η^2 side-by-side mode via four Ag-P bonds, which is similar to that observed in $[Cu_4I_4(dpppda)]_n$ [62]. (Fig. 1)

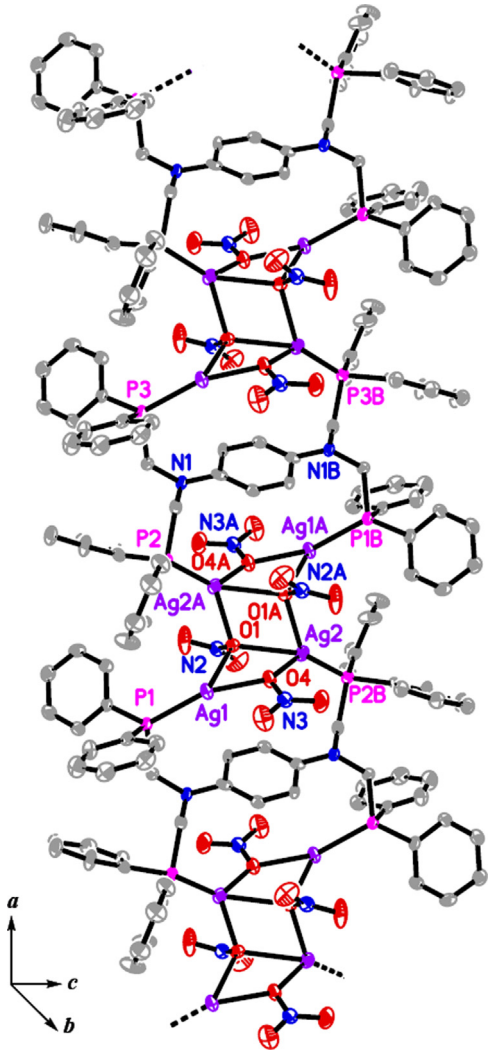

Fig. 1. View of a section of the 1D chain of **1** extending along the *a* axis. Symmetry codes: A: $1-x, 1-y, 1-z$; B: $2-x, 1-y, 1-z$. All H atoms were omitted for clarity. Selected bond lengths (Å) and angles (°): Ag1-P1 2.213(7), Ag1-O1 2.489(7), Ag1-O4 2.213(7), Ag2-P2 2.341(3), Ag2-O1 2.406(7), Ag2-O4 2.398(7), O4-Ag1-P(1) 159.2(2), O4-Ag1-O1 71.2(2), P1-Ag1-O1 128.04(17), O1-Ag2-O1 72.5(3), O4-Ag2-O1, 78.8(3), P2-Ag2-O1 140.91(19), P2-Ag2-O4 134.5(2).

3.2. Optical properties of *1*

The optical absorption and diffuse-reflection spectrum of crystalline solid **1** was measured at ambient temperature. The correlated solid-state UV spectrum showed the maxima absorption at 355 nm (Fig. S4). The band gap energy (Eg) of **1** was determined by the Kubelka–Munk method [63] based on the diffuse reflectance spectra. The energy data were calculated by:

$$E = \frac{1240}{\lambda}$$

The *K-F* data were calculated from the reflectance using the Kubelka–Munk function:

$$K - F = \frac{(1-R)^2}{2R}$$

where λ is the wavelength, and *R* is the reflectance at a given energy. The energy band gap (E_{onset}) obtained by extrapolation of the linear portion of the absorption edges was estimated to be 2.78 eV, implying that **1** possesses the nature of semiconductivity [43,44] (Fig. 2). This value suggested that **1** may response to UV light and have the potential capacity for catalyzing the photodegradation reactions. Thus a high pressure Hg lamp (λ_{max} = 365 nm) was employed in the following photodegradation reactions. (Fig. 2)

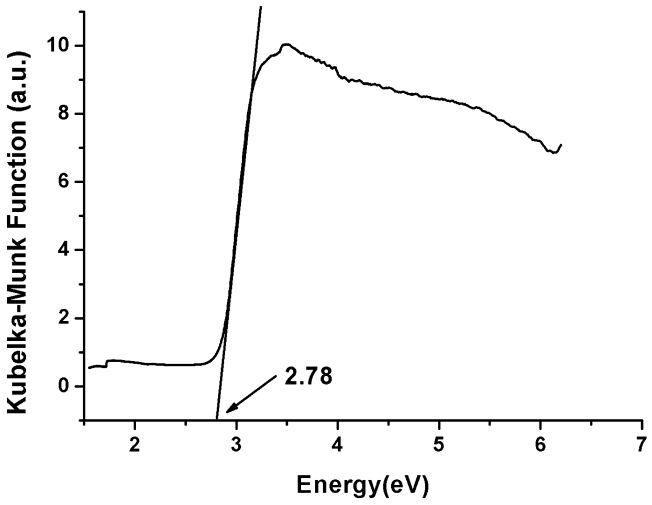

Fig. 2. Solid-state optical diffuse-reflection spectrum of **1** derived from diffuse reflectance data at ambient temperature.

3.3. Photodegradation reactions catalyzed by *1*

The catalytic activity of **1** was evaluated by the photodegradation of NB, PNP or 2,4-DNP in aqueous solution (5×10^{-4} M). The decomposition of NB, PNP or 2,4-DNP was monitored by the characteristic absorption band at 267 nm for NB, 317 nm for PNP or 356 nm for 2,4-DNP. As shown in Fig. 3, each of the three nitroacromatics was all decomposed completely in the presence of **1** after UV light irradiation for 5 h (for NB and PNP) and 6 h (for 2,4-DNP). The decrease of the concentration of each nitroaromatic was negligible (Fig. S5 and Fig. S6) when the solution of each nitroaromatic without **1** was irradiated by UV light under the same conditions or when the mixture containing **1** and each nitroaromatic were stirred in the dark for 10 h. These results showed that in both cases there was no evident reaction between **1** and each nitroaromatic, but both **1** and the UV light irradiation were indispensable in the photodegradation. (Fig. 3)

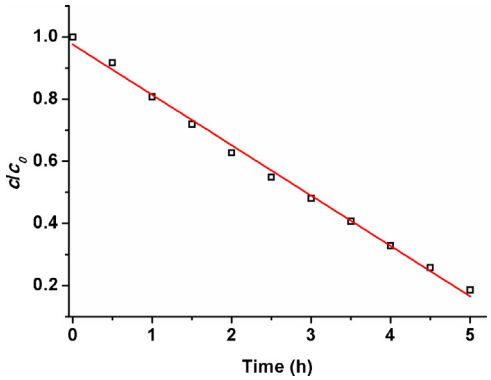

Fig. 4. Pseudo-zero-order plot for the photodegradation of NB in the presence of **1** under UV light irradiation. The square dots and the red line represent the experimental data and the fitted least-square line, respectively.

3.4. Kinetics of the catalytic photodegradation reaction

The kinetics of the photodegradation reaction of NB, PNP or 2,4-DNP catalyzed by **1** was further studied. As shown in Fig. 4 and Fig. S7, the concentration of the remaining nitroaromatic was decreased regularly as the irradiation time was prolonged. This curve followed a pseudo-zero-order kinetics character, implying that such a catalytic photodegradation reaction might take place at the surface of **1**. The zero-order kinetics model could be expressed by:

$$c = c_0 - kt$$

where c_0 and c are the initial and the remaining concentrations of each nitroaromatic at regular time intervals, respectively. k is the apparent zero-order rate constant. The fitted lines in Fig. 4 were generated by the least square method, of which the slope was

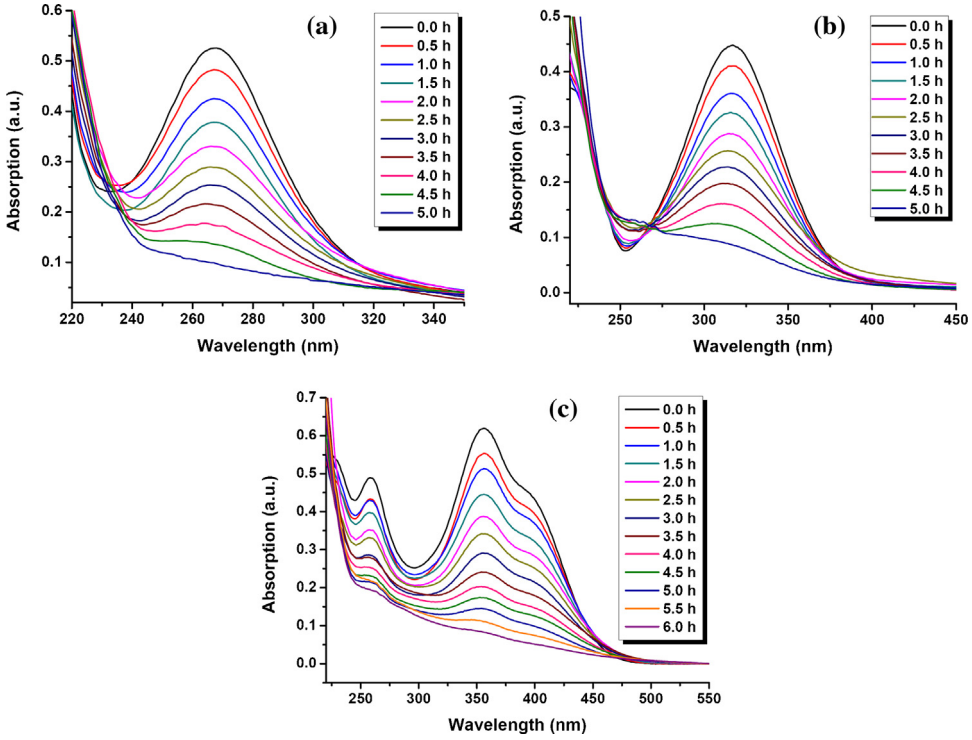

Fig. 3. UV–vis spectra of NB (a), PNP (b) and 2,4-DNP (c) solutions in the presence of **1** under UV irradiation at different time intervals.

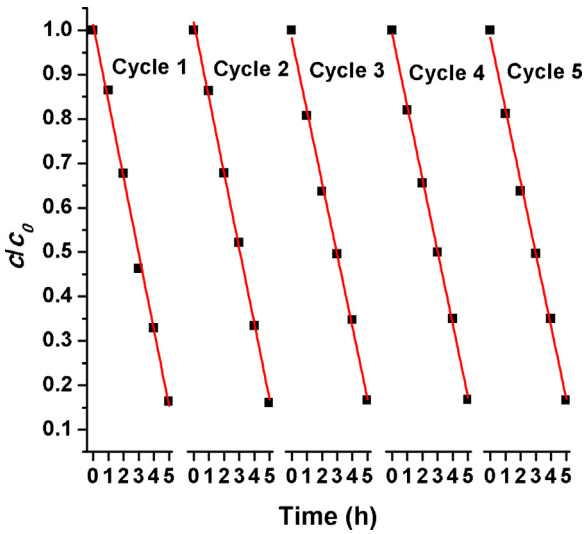

Fig. 5. The repeated catalytic performance of **1** for the photodegradation of NB in water under UV light irradiation. The square dots and the red line are the experimental data and the fitted least-square line, respectively.

$-k/c_0$. Thus the k values were calculated to be 0.81×10^{-4} (NB), 0.79×10^{-4} (PNP) and 0.73×10^{-4} (2,4-DNP) mol·L^{-1}·h^{-1}, respectively. There have been few zero-order reaction examples involved in the photodegradation of NB. For example, Whang et al. reported that the photodegradation of NB catalyzed by TiO_2 nanoparticles coated on a quartz tube [64] was confirmed to be the zero-order reaction with the k value of 2.69×10^{-4} mol·L^{-1}·h^{-1}. This k value was *ca.* 3 times larger than those reported in this work. Compared with many known first-order reactions, the pseudo-zero-order reactions catalyzed by **1** were somewhat slower than those initialized by TiO_2 (3 h for NPs) [65], nanocrystalline Mg-Mn ferrites (4 h for NB) [66], but comparable to that catalyzed by iron (5 h for NB) [67]. The catalytic activities of **1** and TiO_2 (Degussa P-25) were compared by control experiments. Under the catalysis of TiO_2, the three nitroacromatics were completely decomposed after taking longer irradiation time (7.5 h for NB, 5 h for PNP and 7 h for 2,4-DNP) (Fig. S8), which indicated that **1** had a better catalytic activity than TiO_2 under the same experimental conditions. (Fig. 4)

3.5. Reusability of the photocatalyst *1*

Catalyst **1** seemed quite stable during the photodegradation reaction and could be readily separated by centrifugation and recycled by adding it into the freshly-prepared solution of each nitroaromatic to renew the photodegradation reaction. The concentration of each nitroaromatic in water remained decreased regularly even after the 5 cycles (Fig. 5 for NB, Fig. S8 for PNP and 2,4-DNP). The PXRD patterns of the photocatalyst **1** separated after cycle 1 and cycle 5 (Fig S3) matched well with those generated by single-crystal X-ray diffraction data of **1**. All these results demonstrated that **1** retained good catalytic efficiency after the fifth cycle reaction. (Fig. 5)

To confirm that **1** worked as an efficient catalyst for the photodegradation of the three nitroaromatics, we examined the SEM images of solid **1** before and after UV irradiation (Fig. 6). The surfaces of solid **1** before and after UV irradiation were quite similar, which, along with the PXRD results mentioned above, suggested that no catalyst/nitroaromatic composite was formed during the degradation process. Could such a degradation reaction be catalyzed by any water-soluble components generated by the reaction of **1** and the nitroaromatic in water? Firstly, we mixed **1** and the nitroaromatic in water in the dark. The resulting mixture was stirred for several hours and then filtered. The filtrate was irradiated by UV light, resulting in no noticeable degradation of the nitroaromatic in water (Fig. S10). Secondly, after the photodegradation reaction, the mixture was filtered and the same amount of nitroaromatic was re-added into the filtrate. Irradiating the resulting solution with UV light led to no appreciable degradation of nitroaromatic in water (Fig. S11). Both results suggested that there were no active catalytic components (e.g. Ag^+ ion) formed in the

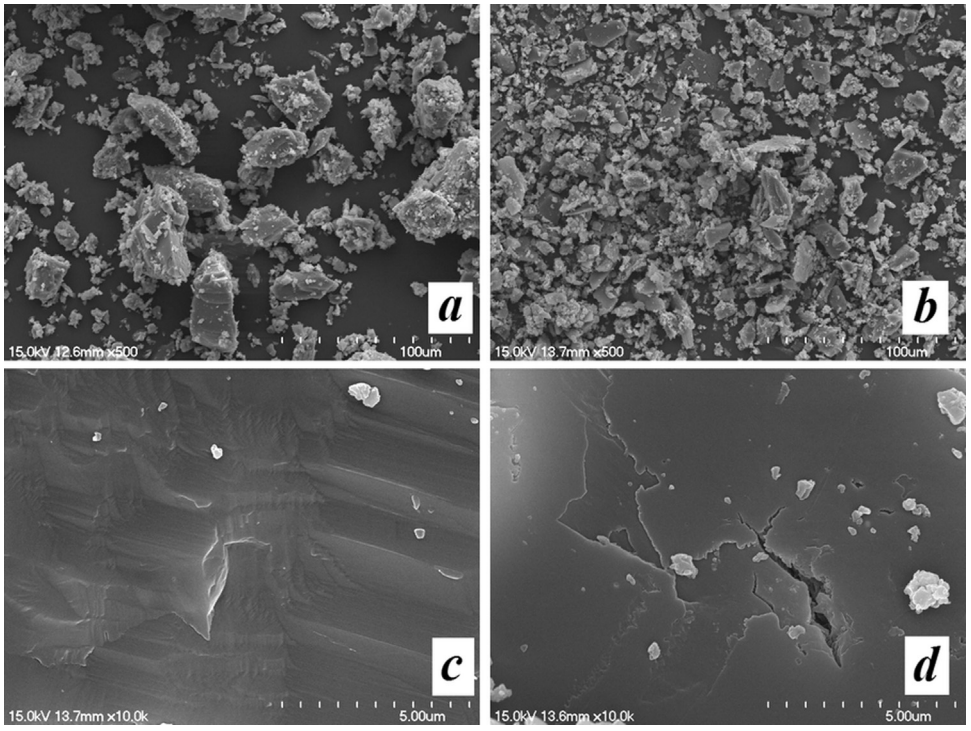

Fig. 6. SEM images of **1** before (a, c) and after (b, d) irradiation.

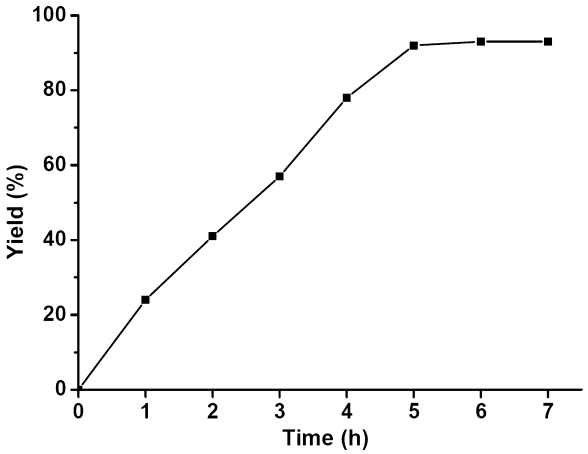

Fig. 7. The yields of CO_2 (based on NB) generated from the photodegradation of NB catalysed by **1** within 7 h.

water phase containing catalyst **1** and the nitroaromatic before and after the photodegradation. In addition, control experiments revealed that neither dpppda nor $AgNO_3$ could catalyze such a photodegradation under the same conditions because no decrease in the concentration of the nitroaromatic was detected (Fig. S12 and Fig. S13). (Fig. 6)

3.6. The proposed mechanism for the photodegradation reaction

The mechanism of the photodegradation of organic pollutants catalyzed by semiconductive materials was once reported by Chen and Paola (Scheme S1) [12,17]. The irradiation of UV light excited electrons (e^-) from the valence band (VB) to the conduction band (CB), yielding the same amount of holes (h^+). The key intermediate, hydroxyl radical ($^\bullet OH$), was generated by the combination of H^+ with $O_2^{\bullet -}$ generated from the reduction of O_2 by e^- as well as the oxidation of OH^- oxidized by h^+. The $^\bullet OH$ radical was so active as to destroy the organic compounds into CO_2, H_2O and other products. As discussed earlier in this paper, the band gap (2.78 eV) of **1** was in the range of semiconductors. Therefore the photodegradation described in this work was assumed to hold the similar mechanism. To affirm this hypothesis, we selected NB as a model compound. It is well known that *tert*-butyl alcohol (TBA) is an effective quenching agent for the $^\bullet OH$ radical and could be used as a scavenger to capture radicals in some systems via the following reaction [68–70].

$$^\bullet OH + t\text{-BuOH} \rightarrow t\text{-BuOH}^\bullet$$

Thus when excess TBA (0.2 mL) was added into the suspension containing **1** and NB, the photodegradation of NB was evidently blocked as the UV light irradiation of 5 h could lead to the decomposition of only 10% NB (Fig. S14), suggesting a $^\bullet OH$ radical-mediated mechanism. Another attempt to probe the mechanism was carried out by collecting the final photodegradation products. Firstly, the resulting solution after photodegradation was extracted by acetic ether, and the resulting organic phase was analyzed by gas chromatography (GC). No organic species were detected, implying that NB was completely decomposed. Secondly, the proposed CO_2 evolved from the reaction was collected by hanging a small bottle of saturated $Ba(OH)_2$ solution inside the reaction tube loaded with a suspension of **1** and NB under O_2 atmosphere (Fig. S2). After the irradiation, white $BaCO_3$ precipitate was observed, which was collected, dried and weighed to calculate the yield of CO_2. Seven consecutive reactions were performed and were stopped by moving the tubes out of the reaction system every 1 h. As shown in Fig. 7, the yield of CO_2 (based on NB) was increased from 25% to 92% as the irradiation time was elongated from 1 h to 5 h. After 6 h, it reached the maximum yield (93%). This result was also consistent with the pseudo-zero-order kinetics of the photodegradation of NB and the $^\bullet OH$ radical-mediated mechanism. Intriguingly, analogous reactions under N_2 atmosphere could lead to the photodegradation of NB in water, but no CO_2 was detected. The LC-MS analysis of the resulting solution revealed complicated peaks, whose identities could not be identified accurately. (Fig. 7)

4. Conclusions

In summary, we demonstrated the design and synthesis of the Ag(I)/tetraphosphine coordination polymer **1**. Complex **1** has a 1D chain structure in which the chair-like $[Ag_4(NO_3)_4]$ fragments are linked by dpppda ligands in a Z-shaped μ-η^2:η^2 side-by-side mode. Compound **1** represented the first example of a 1D coordination polymer that exhibited good catalytic performance in the degradation of three nitroaromatics (NB, PNP and 2,4-DNP) in aqueous solutions under UV irradiation. The photodegradation reactions reported in this article adopted an uncommon pseudo-zero-order kinetics. Such catalytic photodegradations were supposed to take a $^\bullet OH$ radical-mediated mechanism, which led to the complete decomposition of the nitroaromatic in water accompanying the almost quantitative evolution of CO_2. In addition, catalyst **1** was quite stable and showed no obvious catalytic efficiency decay after 5 cycles. Further studies on exploring the photocatalytic activity of **1** towards other organic toxic materials such as organic dyes and aromatic halides in industrial wastewaters are under way. The methodology reported here could be applied to prepare other polydimensional Ag(I) coordination polymers of polyphosphine ligands with new structures and better catalytic performance for the photodegradation of nitroaromatics in polluted waters.

Acknowledgements

The authors thank the financial supports from by the National Natural Science Foundation of China (21271134, 21171124 and 21373142) and the State Key Laboratory of Organometallic Chemistry of Shanghai Institute of Organic Chemistry (2015kf-07). J.P. Lang also highly appreciates the financial supports from the Qing-Lan Project and the "333" Project of Jiangsu Province, the Priority Academic Program Development of Jiangsu Higher Education Institutions, and the "SooChow Scholar" Program of Soochow University. The authors greatly thank the helpful comments from the editor and the reviewers.

Appendix A. Supplementary data

CCDC 1,001,763 contains the supplementary crystallographic data for **1**. These data can be obtained free of charge from the Cambridge Crystallographic Data Centre via http://www.ccdc.cam.ac.uk/data_request/cif. Supplementary data associated with this article can be found, in the online version, at http://dx.doi.org/10.1016/j.apcatb.2014.12.024.

References

[1] E. Bizani, K. Fytianos, I. Poulios, V. Tsiridis, J. Hazard. Mater. 136 (2006) 85–94.
[2] G.M. ElShafei, F.Z. Yehia, O.I. Dimitry, A.M. Badawi, G. Eshaq, Ultrason. Sonochem. 21 (2014) 1358–1365.
[3] X.T. Shen, L.H. Zhu, N. Wang, T. Zhang, H.Q. Tang, Catal. Today 225 (2014) 164–170.
[4] K.Y. Xia, F.C. Xie, Y. Ma, Ultrason. Sonochem. 21 (2014) 549–553.
[5] S.H. Yu, J. Hu, J.L. Wang, Radiat. Phys. Chem. 79 (2010) 1039–1046.
[6] B.X. Zhao, G. Mele, I. Pio, J. Li, L. Palmisano, G. Vasapollo, J. Hazard. Mater. 176 (2010) 569–574.
[7] J.J. Pan, B.H. Guan, J. Hazard. Mater. 183 (2010) 341–346.
[8] S. Contreras, M. Rodríguez, E. Chamarro, S. Esplugas, J. Photochem. Photobiol. A: Chem. 142 (2001) 79–83.

[9] L.S. Bell, J.F. Devlin, R.W. Gillham, P.J. Binning, J. Contam. Hydrol. 66 (2003) 201–217.
[10] G. Palmisano, M. Addamo, V. Augugliaro, T. Caronna, A.D. Paola, E.G. López, V. Loddo, G. Marcì, L. Palmisano, M. Schiavello, Catal. Today 122 (2007) 118–127.
[11] X.L. Hu, G.S. Li, J.C. Yu, Langmuir 26 (2010) 3031–3039.
[12] C.C. Chen, W.H. Ma, J.C. Zhao, Chem. Soc. Rev. 39 (2010) 4206–4219.
[13] H. Zhang, D. Chen, X.J. Lv, Y. Wang, H.X. Chang, J.H. Li, Environ. Sci. Technol. 44 (2010) 1107–1111.
[14] M.J. López-Muñoz, J. Aguado, A. Arencibia, R. Pascual, Appl. Catal. B: Environ. 104 (2011) 220–228.
[15] H. Zhang, X.J. Lv, Y.M. Li, Y. Wang, J.H. Li, ACS Nano 4 (2009) 380–386.
[16] T.R. Gordon, M. Cargnello, T. Paik, F. Mangolini, R.T. Weber, P. Fornasiero, C.B. Murray, J. Am. Chem. Soc. 134 (2012) 6751–6761.
[17] A.D. Paola, E. Garcia-Lopez, G. Marci, L. Palmisano, J. Hazard. Mater. 211–212 (2012) 3–29.
[18] M.H. Priya, G. Madras, J. Photochem. Photobiol. A: Chem. 178 (2006) 1–7.
[19] M. Andersson, H. Birkedal, N.R. Franklin, T. Ostomel, S. Boettcher, A.E. Palmqvist, G.D. Stucky, Chem. Mater. 17 (2005) 1409–1415.
[20] T. Arai, M. Yanagida, Y. Konishi, Y. Iwasaki, H. Sugihara, K. Sayama, J. Phys. Chem. C 111 (2007) 7574–7577.
[21] J.W. Tang, Z.G. Zou, J.H. Ye, Angew. Chem. Int. Ed. 43 (2004) 4463–4466.
[22] A. Fuerte, M.D. Hernández-Alonso, A.J. Maira, A. Martínez-Arias, M. Fernández-García, J.C. Conesa, J. Soria, Chem. Commun. (2001) 2718–2719.
[23] W. Zhao, C.C. Chen, X.Z. Li, J.C. Zhao, H. Hidaka, N. Serpone, J. Phys. Chem. B 106 (2002) 5022–5028.
[24] J.J. Testa, M.A. Grela, M.I. Litter, Langmuir 17 (2001) 3515–3517.
[25] H. Kato, H. Kobayashi, A. Kudo, J. Phys. Chem. B 106 (2002) 12441–12447.
[26] M. Iwasaki, M. Hara, H. Kawada, H. Tada, S. Ito, J. Colloid Interface Sci. 224 (2000) 202–204.
[27] H. Irie, Y. Watanabe, K. Hashimoto, J. Phys. Chem. B 107 (2003) 5483–5486.
[28] S. Sakthivel, M. Janczarek, H. Kisch, J. Phys. Chem. B 108 (2004) 19384–19387.
[29] X.T. Hong, Z.P. Wang, W.M. Cai, F. Lu, J. Zhang, Y.Z. Yang, N. Ma, Y.J. Liu, Chem. Mater. 17 (2005) 1548–1552.
[30] S. Sakthivel, H. Kisch, Angew. Chem. Int. Ed. 42 (2003) 4908–4911.
[31] Y.L. Hou, R.W.Y. Sun, X.P. Zhou, J.H. Wang, D. Li, Chem. Commun. 50 (2014) 2295–2297.
[32] Y.Q. Chen, S.J. Liu, Y.W. Li, G.R. Li, K.H. He, Y.K. Qu, T.L. Hu, X.H. Bu, Cryst. Growth Des. 12 (2012) 5426–5431.
[33] T. Wen, D.X. Zhang, J. Liu, R. Lin, J. Zhang, Chem. Commun. 49 (2013) 5660–5662.
[34] Y.Q. Chen, G.R. Li, Y.K. Qu, Y.H. Zhang, K.H. He, Q. Gao, X.H. Bu, Cryst. Growth Des. 13 (2013) 901–907.
[35] X.L. Wang, J. Luan, F.F. Sui, H.Y. Lin, G.C. Liu, C. Xu, Cryst. Growth Des. 13 (2013) 3561–3576.
[36] J.S. Hu, Y.J. Shang, X.Q. Yao, L. Qin, Y.Z. Li, Z.J. Guo, H.G. Zheng, Z.L. Xue, Cryst. Growth Des. 10 (2010) 4135–4142.
[37] X.L. Wang, Q. Gao, A.X. Tian, G.C. Liu, Cryst. Growth Des. 12 (2012) 2346–2354.
[38] X. Wang, M.M. Zhang, X.L. Hao, Y.H. Wang, Y. Wei, F.S. Liang, L.J. Xu, Y.G. Li, Cryst. Growth Des. 13 (2013) 3454–3462.
[39] L.L. Wen, J.B. Zhao, K.L. Lü, Y.H. Wu, K.J. Deng, X.K. Leng, D.F. Li, Cryst. Growth Des. 12 (2012) 1603–1612.
[40] Q. Wu, W.L. Chen, D. Liu, C. Liang, Y.G. Li, S.W. Lin, E. Wang, Dalton Trans. 40 (2011) 56–61.
[41] Y. Hu, F. Luo, F. Dong, Chem. Commun. 47 (2011) 761–763.
[42] J. Guo, J.F. Ma, J.J. Li, J. Yang, S.X. Xing, Cryst. Growth Des. 12 (2012) 6074–6082.
[43] D.X. Li, C.Y. Ni, M.M. Chen, M. Dai, W.H. Zhang, W.Y. Yan, H.X. Qi, Z.G. Ren, J.P. Lang, CrystEngComm 16 (2014) 2158–2167.
[44] M. Dai, X.R. Su, X. Wang, B. Wu, Z.G. Ren, X. Zhou, J.P. Lang, Cryst. Growth Des. 14 (2014) 240–248.
[45] T. Wen, D.X. Zhang, J. Zhang, Inorg. Chem. 52 (2013) 12–14.
[46] A. Khanna, V. Shetty, Environ. Sci. Pollut. Res. 20 (2013) 5692–5707.
[47] Z.G. Yi, J.H. Ye, N. Kikugawa, T. Kako, S.X. Ouyang, H. Stuart-Williams, H. Yang, J.Y. Cao, W.J. Luo, Z.S. Li, Y. Liu, R.L. Withers, Nat. Mater. 9 (2010) 559–564.
[48] S.S. Ma, J.J. Xue, Y.M. Zhou, Z.W. Zhang, J. Mater. Chem. A 2 (2014) 7272–7280.
[49] M. Ge, N. Zhu, Y.P. Zhao, J. Li, L. Liu, Ind. Eng. Chem. Res. 51 (2012) 5167–5173.
[50] R.S. Patil, M.R. Kokate, D.V. Shinde, S.S. Kolekar, S.H. Han, Spectrochim. Acta A 122 (2014) 113–117.
[51] M. Wałęsa-Chorab, V. Patroniak, M. Kubicki, G. Kądziołka, J. Przepiórski, B. Michalkiewicz, J. Catal. 291 (2012) 1–8.
[52] J.H. Yang, X.Y. Wu, R.T. He, Z.G. Ren, H.X. Li, H.F. Wang, J.P. Lang, Cryst. Growth Des. 13 (2013) 2124–2134.
[53] S. Sun, Z.G. Ren, J.H. Yang, R.T. He, F. Wang, X.Y. Wu, W.J. Gong, H.X. Li, J.P. Lang, Dalton Trans. 41 (2012) 8447–8454.
[54] N.Y. Li, Z.G. Ren, D. Liu, R.X. Yuan, L.P. Wei, L. Zhang, H.X. Li, J.P. Lang, Dalton Trans. 39 (2010) 4213–4222.
[55] X.Y. Wu, Z.G. Ren, J.P. Lang, Dalton Trans. 43 (2014) 1716–1723.
[56] D. Liu, Z.G. Ren, H.X. Li, J.P. Lang, N.Y. Li, B.F. Abrahams, Angew. Chem. Int. Ed. 49 (2010) 4767–4770.
[57] D. Liu, J.P. Lang, B.F. Abrahams, J. Am. Chem. Soc. 133 (2011) 11042–11045.
[58] F. Wang, C.Y. Ni, Q. Liu, F.L. Li, J. Shi, H.X. Li, J.P. Lang, Chem. Commun. 49 (2013) 9248–9250.
[59] Q.L. Ni, Y.F. Liao, C.Y. Ge, L.C. Gui, L.H. Tang, X.J. Wang, Chem. Res. Appl. 5 (2008) 617–620.
[60] G.M. Sheldrick, SHELXS-97, Program for Solution of Crystal Structures, University of Göttingen, Germany, 1997.
[61] G.M. Sheldrick, SHELXL-97, Program for Refinement of Crystal Structures, University of Göttingen, Germany, 1997.
[62] N.Y. Li, Z.G. Ren, D. Liu, J. Wang, M. Dai, H.X. Li, J.P. Lang, Inorg. Chem. Commun. 12 (2009) 1031–1034.
[63] C. Wang, Z.G. Xie, K.E. deKrafft, W.B. Lin, J. Am. Chem. Soc. 133 (2011) 13445–13454.
[64] T.J. Whang, M.T. Hsieh, T.E. Shi, C.H. Kuei, Int. J. Photoenergy (2014), http://dx.doi.org/10.1155/2012/681941.
[65] K. Tanaka, W. Luesaiwong, T. Hisanaga, J. Mol. Catal. A 122 (1997) 67–74.
[66] T.K. Pathak, N.H. Vasoya, T.S. Natarajan, K.B. Modi, R.J. Tayade, Mater. Sci. Forum 764 (2013) 116–129.
[67] Y. Mu, H.Q. Yu, J.C. Zheng, S.J. Zhang, G.P. Sheng, Chemosphere 54 (2004) 789–794.
[68] S. Zheng, W.J. Jiang, Y. Cai, D.D. Dionysiouc, K.E. O'shea, Catal. Today 224 (2014) 83–88.
[69] B. Subramanian, Q. Yang, Q. Yang, A.P. Khodadoust, D.D. Dionysiou, J. Photochem. Photobiol. A: Chem. 192 (2007) 114–121.
[70] A. Marcinek, J. Zielonka, J.Gñ. Ebicki, C.M. Gordon, I.R. Dunkin, J. Phys. Chem. A 105 (2001) 9305–9309.